

Published in final edited form as:

*Dent Mater.* 2013 February ; 29(2): 231–240. doi:10.1016/j.dental.2012.10.010.

## Novel calcium phosphate nanocomposite with caries-inhibition in a human *in situ* model

Mary Anne S. Melo<sup>1,2</sup>, Michael D. Weir<sup>1</sup>, Lidiary K.A. Rodrigues<sup>2</sup>, and Hockin H.K. Xu<sup>1,3,4,5</sup>

<sup>1</sup>Biomaterials & Tissue Engineering Division, Dept. of Endodontics, Prosthodontics and Operative Dentistry, University of Maryland Dental School, Baltimore, MD 21201, USA

<sup>2</sup>Faculty of Pharmacy, Dentistry and Nursing, Federal University of Ceara, Fortaleza, CE, Brazil

<sup>3</sup>Center for Stem Cell Biology & Regenerative Medicine, University of Maryland School of Medicine, Baltimore, MD 21201, USA

<sup>4</sup>Marlene and Stewart Greenebaum Cancer Center, University of Maryland School of Medicine, Baltimore, MD 21201, USA

<sup>5</sup>Department of Mechanical Engineering, University of Maryland, Baltimore County, MD 21250, USA

### Abstract

**Objectives**—Secondary caries at the restoration margins remains the main reason for failure. Although calcium phosphate (CaP) composites are promising for caries inhibition, there has been no report of CaP composite to inhibit caries *in situ*. The objectives of this study were to investigate the caries-inhibition effect of nanocomposite containing nanoparticles of amorphous calcium phosphate (NACP) in a human *in situ* model for the first time, and to determine colony-forming units (CFU) and Ca and P ion concentrations of biofilms on the composite restorations.

**Methods**—NACP with a mean particle size of 116 nm were synthesized via a spray-drying technique. Two composites were fabricated: NACP nanocomposite, and control composite filled with glass particles. Twenty-five volunteers wore palatal devices containing bovine enamel slabs with cavities restored with NACP or control composite. After 14 days, the adherent biofilms were collected for analyses. Transverse microradiography determined the enamel mineral profiles at the margins, and the enamel mineral loss ! Z was measured.

**Results**—NACP nanocomposite released Ca and P ions and the release significantly increased at cariogenic low pH ( $p < 0.05$ ). Biofilms on NACP nanocomposite contained higher Ca ( $p = 0.007$ ) and P ions ( $p = 0.005$ ) than those of control ( $n = 25$ ). There was no significant difference in biofilm CFU between the two composites ( $p > 0.1$ ). Microradiographs showed typical subsurface lesions in enamel next to control composite, but much less lesion around NACP nanocomposite. Enamel mineral loss ! Z (mean  $\pm$  sd;  $n = 25$ ) around NACP nanocomposite was  $13.8 \pm 9.3 \mu\text{m}$ , much less than  $33.5 \pm 19.0 \mu\text{m}$  of the control ( $p = 0.001$ ).

© 2004 Academy of Dental Materials. Published by Elsevier Ltd. All rights reserved.

Correspondence: Prof. Lidiary K. A. Rodrigues (lidiarykarla@yahoo.com), Faculty of Pharmacy, Dentistry and Nursing, Federal University of Ceara, Fortaleza, CE, Brazil., Prof. Hockin H. K. Xu (hxu@umaryland.edu), Director of Biomaterials & Tissue Engineering Division, Department of Endodontics, Prosthodontics and Operative Dentistry, University of Maryland Dental School, Baltimore, MD 21201.

**Publisher's Disclaimer:** This is a PDF file of an unedited manuscript that has been accepted for publication. As a service to our customers we are providing this early version of the manuscript. The manuscript will undergo copyediting, typesetting, and review of the resulting proof before it is published in its final citable form. Please note that during the production process errors may be discovered which could affect the content, and all legal disclaimers that apply to the journal pertain.

**Significance**—Novel NACP nanocomposite substantially reduced caries formation in a human in situ model for the first time. Enamel mineral loss at the margins around NACP nanocomposite was less than half of the mineral loss around control composite. Therefore, the Ca and P ion-releasing NACP nanocomposite is promising for caries-inhibiting restorations.

## Keywords

human in situ model; dental nanocomposite; calcium phosphate nanoparticles; dental biofilms; ion release; secondary caries inhibition

## 1. Introduction

Dental composites consisting of fillers in a resin matrix are increasingly used because of their esthetics and enhanced performance [1-7]. Extensive efforts have been performed to improve the resin compositions, filler reinforcement, and polymerization properties [8-15]. However, secondary caries remains a main challenge facing composite restorations [16-18]. Caries at the restoration margins is a frequent reason for replacement of existing restorations [19]. The replacement of the failed restorations accounts for 50% to 70% of all restorations performed [20]. Replacement dentistry costs \$5 billion annually in the U.S. [21]. To inhibit caries around the restorations, calcium phosphate (CaP)-resin composite materials were developed, which were shown to be effective in remineralizing tooth lesions in vitro [22-25]. However, to date, the caries-inhibition efficacy of CaP composite in a human in situ model has not been reported.

Traditional CaP composites were developed by filling micrometer-sized CaP particles into dental resins [22,23]. For example, amorphous calcium phosphate (ACP,  $\text{Ca}_3[\text{PO}_4]_2$ ) particles with a mean size of 55  $\mu\text{m}$  were filled into resins [23]. ACP is a precursor that forms initially and then transforms to apatite. Hydroxyapatite,  $\text{Ca}_{10}(\text{PO}_4)_6(\text{OH})_2$ , the prototype of minerals in teeth/bones, is the final stable product in the precipitation of calcium and phosphate ions in neutral and basic solutions [26]. Traditional ACP composite released supersaturating levels of calcium phosphate ions and remineralized enamel lesions in vitro [23]. However, traditional calcium phosphate composites were mechanically weak and not suitable for bulk restoratives [22,23]. Recently, novel nanocomposites were developed with nanoparticles of ACP (NACP) having a mean particle size of 116 nm [27]. The NACP nanocomposite released calcium and phosphate ions similar to traditional CaP composites, but with a 2-fold increase in flexural strength and elastic modulus for load-bearing restorations [27]. The flexural strength and elastic modulus of the NACP nanocomposite matched those of a commercial composite control [27]. Furthermore, NACP nanocomposite effectively neutralized a lactic acid challenge, while commercial control restoratives failed to neutralize the acid [28]. However, the caries inhibition capability of the NACP nanocomposite in teeth has not been investigated.

Therefore, the objective of this study was to investigate the effects of NACP nanocomposite on caries inhibition in situ in the oral environment for the first time. A randomized split-mouth design was conducted with 25 volunteers wearing palatal devices for 14 days. After 14 days, the samples were removed, the biofilms were analyzed for Ca and P ion concentrations, and mineral content in enamel was measured via transverse microradiography. It was hypothesized that: (1) NACP nanocomposite will increase the Ca and P ion concentrations in biofilms in situ; (2) NACP nanocomposite will inhibit enamel caries at the enamel-composite interface to yield much less mineral loss, compared to control composite without NACP fillers.

## 2. Materials and Methods

### 2.1 NACP nanocomposite fabrication

A spray-drying technique was developed to synthesize calcium phosphate and calcium fluoride nanoparticles [29,30]. To make NACP, a solution was prepared using 1.5125 g of acetic acid (Baker, Phillipsburg, NJ), 0.8 g of calcium carbonate (Fisher, Fair Lawn, NJ) and 5.094 g of dicalcium phosphate-anhydrous with water. The calcium and phosphate concentrations in the solution were 8 and 5.333 mmol/L, respectively. The solution was sprayed through a nozzle into a heated chamber. The water and volatile acid were evaporated and the dried particles were collected by an electrostatic precipitator (AirQuality, Minneapolis, MN). This method yielded NACP with a mean particle size of 116 nm as measured in a previous study [27].

A monomer consisting of Bis-GMA (bisphenol-glycidyl dimethacrylate) and TEGDMA (triethylene glycol dimethacrylate) at 1:1 ratio (all by mass) was rendered light-curable with 0.2% camphorquinone and 0.8% ethyl 4-N,N-dimethylaminobenzoate. As reinforcement co-fillers, barium-boroaluminosilicate glass particles with a median diameter of 1.4  $\mu\text{m}$  (Caulk/Dentsply, Milford, DE) were silanized with 4% 3 methacryloxypropyltrimethoxysilane and 2% n-propylamine [31]. The fillers were mixed with the resin at a total filler mass fraction of 60% to form a cohesive paste. Two composites were fabricated with fillers of: (1) 40% NACP + 20% glass (NACP nanocomposite); and (2) 0% NACP + 60% glass (control composite).

### 2.2. Calcium (Ca) and phosphate (P) ion release measurement

Ca and P ion release from the NACP nanocomposite was measured. The composite paste was placed into rectangular molds of  $2 \times 2 \times 12$  mm following previous studies [29,31]. The specimens were photo-cured (Triad 2000, Dentsply, York, PA) in air for 1 min on each side, and then incubated at 37 °C in a humidifier for 1 d. A sodium chloride solution (133 mmol/L) was buffered to three pH values: pH 4 with 50 mmol/L lactic acid, pH 5.5 with 50 mmol/L acetic acid, and pH 7 with 50 mmol/L HEPES. Following previous studies [29,31], three specimens of approximately  $2 \times 2 \times 12$  mm<sup>3</sup> were immersed in 50 mL of solution at each pH, yielding a specimen volume/solution of 2.9 mm<sup>3</sup>/mL. This compared to a specimen volume per solution of approximately 3.0 mm<sup>3</sup>/mL in a previous study [32]. At 1, 2, 3, 5, 7, 10, 14, 21, and 28 d, aliquots of 0.5 mL were removed and replaced by fresh solution. Ca and P ion concentrations at each time period were measured via a spectrophotometric method (DMS-80 UV-visible, Varian, Palo Alto, CA) using known standards and calibration curves [22,23,32].

### 2.3. In situ tooth demineralization model

The *in situ* model of the present study was approved by the Research and Ethics Committee of the Federal University of Ceará in Brazil (Protocol # 028/2011) and conformed to the Resolution 196/96 of the National Health Council concerning the Human Research Code of Ethics. This *in situ* model was similar to those reported in previous studies which successfully enabled the investigation of enamel and dentin caries formation [33-36]. All participants signed written informed consent before being accepted into the study. Twenty-five volunteers were selected who fulfilled the following inclusion criteria: Normal salivary flow rate, stimulated-saliva buffering capacity, good general and oral health with no active caries lesions or periodontal treatment needs, ability to comply with the experimental protocol, not having used antibiotics during the 3 months prior to the study, and not using fixed or removable orthodontic devices [34-36].

Freshly-extracted bovine teeth were used following previous studies [37-40]. One hundred bovine incisors were used to prepare one hundred enamel slabs ( $5 \times 5 \times 2$  mm) using a diamond saw (Buehler, Lake Bluff, IL), as shown schematically in Fig. 1A. Following a previous study [41], circular cavities with an approximate diameter of 2 mm and a depth of 1.5 mm were prepared (Fig. 1A). The 100 enamel slabs with cavities were randomly divided according to a computer-generated randomization list, into two groups of 50 slabs each: one group was filled with the NACP nanocomposite, and the other group was filled with the control composite. To focus on the effects of composite without interference from adhesive, no adhesive was used. Each composite paste was placed into the cavity and light-activated for 20 sec using a light emitting diode Optilight LD Max (Gnatus, Ribeirão Preto, SP, Brasil) with an output of  $600 \text{ mW/cm}^2$ . All the restored slabs were polished using aluminum oxide disc (Sof-lex disk system, M Dental, St. Paul, MN). As shown in Fig. 1A, an enamel surface area of approximately  $5 \times 1.5$  mm adjacent to the restoration was covered with an acid-resistant varnish to act as a control for mineral loss analysis. The filled enamel slabs were stored in a humidior at a relative humidity of 100% at  $37^\circ\text{C}$  for 24 hours and then used in the in situ model.

For 14 days, the 25 volunteers wore removable acrylic custom-made palatal devices, each containing four enamel slabs: two slabs were restored with the NACP nanocomposite on one side, and two slabs were restored with the control composite on the other side (Fig. 1B). Having slabs with two different treatments on the two opposite sides of the same device enabled them to experience the same oral environment for a fair comparison between the two materials. This method was supported by the absence of cross-contamination shown in previous studies [38,42]. Each slab was covered with a plastic mesh with a 1 mm space, to allow biofilm accumulation and to protect the biofilms from mechanical disturbances [36,41]. As a single-blind test, the volunteers did not know which was control composite or NACP nanocomposite. Seven days prior to the experiment and during the 14 d experiment, the volunteers brushed their teeth with non-fluoridated toothpaste. The purpose of this was to determine the effect of NACP nanocomposite on caries formation without interference from fluoridated toothpastes. In order to provide a cariogenic challenge, eight times daily at predetermined times, the volunteers removed the appliance, dripped one drop of a 20% sucrose solution on each slab, and then placed the appliance back into the mouth, following previous studies [36,41].

#### 2.4. Biofilm analyses

On day 14, 12 h after the last application of the sucrose solution, the biofilm formed on each specimen was collected with sterilized plastic cures. The biofilm was weighed in pre-weighed microcentrifuge tubes and agitated for 2 min in a Disrupter Genie Cell Disruptor (Precision Solutions, Rice Lake, WI). An aliquot of  $50 \mu\text{l}$  of the sonicated suspension was diluted in 0.9% NaCl and serial decimal dilutions were inoculated in triplicate by the drop-counting technique in the following culture media [36,41]: mitis salivarius agar containing 20% sucrose, to determine total streptococci; mitis salivarius agar plus 0.2 bacitracin/mL, to determine mutans streptococci; and Rogosa agar supplemented with 0.13% glacial acetic acid, to determine lactobacilli. The plates were incubated in 10%  $\text{CO}_2$  at  $37^\circ\text{C}$  for 48 h. The colony-forming units (CFU) were counted and the results were expressed as CFU/mg of dental biofilm with wet weight [36,41].

In addition, the Ca and P ion concentrations in the biofilms were also measured. The biofilms were treated with 0.5 M of HCl to extract the acid-soluble whole-biofilm Ca and P ions. "Phosphate (P) ions" and "inorganic phosphorus (Pi)" are interchangeable in the context of the present study. Samples were agitated at 30 rpm for 3 h and centrifuged. The supernatant was collected for Ca and P ion measurement via a spectrophotometric method [33].

## 2.5. Transverse microradiography (TMR) to measure mineral content

For TMR, specimen sections were cut to a thickness of approximately 200  $\mu\text{m}$ , as shown schematically in Fig. 1C. The sections were serially-polished with water-cooled abrasive (320, 600, and 1200-grit  $\text{Al}_2\text{O}_3$  papers, Buehler) to a thickness of 110-130  $\mu\text{m}$ , following a previous study [43]. Contact microradiographs of enamel sections were produced on holographic film (Integraf, Kirkland, WA) exposed to 30-min  $\text{Cu-K}\alpha$  radiation (Faxitron-43855A, Hewlett Packard, McMinnville, OR). Mineral profiles were determined by quantitative analysis of microradiographs using NIS Elements-3.2 (Nikon, NY). Digital imaging captured the gray levels of a rectangular area ( $50 \times 600 \mu\text{m}$ ) of the radiographic image using an intensity resolution of 256 gray levels and a spatial resolution of 1.25  $\mu\text{m}/\text{pixel}$  [23]. Following previous studies [34], the mineral loss ( $\Delta Z$ ) was obtained in the enamel region next to the enamel-composite, at four distances from the enamel-composite interface: 0-50, 50-100, 100-150, 150-200  $\mu\text{m}$ , respectively. In addition, mineral loss  $\Delta Z$  was also calculated for the enamel region of 0-250  $\mu\text{m}$  as a whole [34]. This was done by analyzing the grayscale intensity of the rectangular area of  $250 \times 600 \mu\text{m}$  of enamel next to the composite to obtain the average  $\Delta Z$  for this entire region. Net  $\Delta Z$  was obtained as  $\Delta Z_{\text{exposed}} - \Delta Z_{\text{VarnishCovered}}$  for the same enamel section, where  $\Delta Z_{\text{exposed}}$  was the enamel mineral loss on the side without varnish (Fig. 1C). As shown in the results section,  $\Delta Z_{\text{VarnishCovered}}$  was nearly 0, which indicates sound enamel without demineralization [38]. The unit of the integrated mineral loss  $\Delta Z$  is  $\mu\text{m}$ , because  $100 \mu\text{m} \cdot \text{vol}\% = 1 \mu\text{m}$ , following previous studies [22,23,44].

## 2.6. Statistical analysis

Sample size was determined based on previous data [41], where the required number of participants was determined to be 20, in anticipation of a dropout rate of 10%. This was based on an adequate power of 80% and a defined significance level of 5% ( $p < 0.05$ ). Accordingly, to ensure that this group size was available at the end of the study, 25 volunteers were recruited to compensate for possible dropouts (However, all 25 volunteers completed this study). One-way and two-way analyses-of-variance (ANOVA) were performed to detect the significant effects of the variables. Tukey's multiple comparison procedures were performed at a p value of 0.05.

## 3. Results

The Ca and P ion release from NACP nanocomposite specimens is plotted in Fig. 2 (mean  $\pm$  sd;  $n = 5$ ). Two-way ANOVA showed significant effects of pH and immersion time, with a significant interaction between the two variables ( $p < 0.05$ ). Compared to pH 7, the ion release was slightly higher at pH 5.5, but substantially higher and increased with time at a faster rate at pH 4.

The CFU results of biofilms collected from specimens in situ are plotted in Fig. 3A-C (mean  $\pm$  sd;  $n = 25$ ). Biofilms on NACP nanocomposite and control composite restorations had statistically similar total streptococci, mutans streptococci, and lactobacilli ( $p > 0.1$ ). The Ca and P ion concentrations in biofilms are plotted in Fig. 3D and 3E (mean  $\pm$  sd;  $n = 25$ ). The biofilms adherent on NACP nanocomposite restorations had significantly higher calcium ( $p = 0.007$ ) and phosphate ( $p = 0.005$ ) ion concentrations than those on the control composite.

Fig. 4 shows microradiographs for the exposed enamel without varnish. A representative enamel lesion around the control composite is shown in (A). In contrast, there was much less enamel lesion around the NACP nanocomposite, with an example shown in (B). Representative mineral profiles are shown in (C) and (D), having much larger lesion depth and mineral loss in enamel around the control composite than those around the NACP nanocomposite.



The varnish-covered enamel had no mineral loss, with  $\Delta Z_{\text{VarnishCovered}} = 1.6 \pm 1.9 \mu\text{m}$  around control composite, and  $1.0 \pm 0.8 \mu\text{m}$  around NACP nanocomposite ( $p > 0.1$ ). For the exposed enamel, net  $\Delta Z$  values were measured at four different distances away from the composite-enamel interface, and the results are plotted in Fig. 5. The values at the x-axis indicate the distance of the enamel region away from the enamel-composite interface. Two-way ANOVA showed a significant effect of composite type ( $p < 0.05$ ), but no significant effect of the distance from the enamel-composite interface ( $p > 0.1$ ), with no significant interaction between the two variables ( $p > 0.1$ ). At each distance from the enamel-composite interface, the mineral loss (mean  $\pm$  sd;  $n = 25$ ) was much less around the NACP nanocomposite than those around the control composite ( $p < 0.05$ ).

Because the distance from the composite-enamel interface did not significantly affect the enamel mineral loss in Fig. 5, the enamel region of 0-250  $\mu\text{m}$  was measured as a single area to obtain the average value for each enamel section, and the results are plotted in Fig. 6. The enamel lesion depth around the NACP nanocomposite was significantly less than that around the control composite ( $p = 0.001$ ). The enamel mineral loss (mean  $\pm$  sd;  $n = 25$ )  $\Delta Z_{\text{NACPnanocomposite}} = 13.8 \pm 9.3 \mu\text{m}$ , much less than  $\Delta Z_{\text{ControlComposite}} = 33.5 \pm 19.0 \mu\text{m}$  ( $p = 0.001$ ).

#### 4. Discussion

This study represents the first report on calcium phosphate composite behavior in a human in situ model which demonstrated significant enrichment of biofilms with calcium phosphate ions and effective inhibition of enamel lesions. Previous CaP composite studies focused on measurement of ion release and remineralization in vitro [23,44]. Traditional CaP composites had particles sizes of 1-55  $\mu\text{m}$  [23,44]. In contrast, NACP consisted of individual particles with an average size of 37 nm, and clusters where several individual particles were connected to each other yielding an apparent size of 225 nm [45]. The mean particle size for NACP was 116 nm. As shown in recent studies, nanoparticles had high surface areas and released high levels of ions at relatively low filler levels, thereby making room in the resin for reinforcement glass fillers [27]. This method resulted in mechanical properties of the nanocomposite being 2-3 folds those of traditional CaP composites [46]. Secondary caries shortens restoration longevity and requires replacement of failed restorations, which increases the subsequent restoration size and the complexity of the procedure. Hence, the NACP nanocomposite that greatly inhibited enamel caries in situ is promising to reduce the occurrence of secondary caries.

The human in situ model allowed salivary flow and encompassed the complexity of different volunteers [33-36]. Furthermore, the in situ model enabled biofilm formation with the heterogeneity and complication of biofilms and plaques in vivo. While single species biofilms were often used for in vitro investigations, dental plaque is a complicated ecosystem with about 1,000 bacterial species [47]. In addition, different individuals may have different biofilm compositions and dietary habits. Hence, the present study investigated in situ caries-inhibition via NACP nanocomposite using 25 volunteers. There are several previous in situ studies on fluoride treatments. For example, the effect of fluoride-releasing glass ionomers on bovine dentin caries was investigated in 16 human volunteers [38]. Calcium, phosphate and fluoride ion concentrations in biofilms were significantly affected by exposure to sucrose in situ [33]. Glass ionomer increased the fluoride level in biofilms, thereby decreasing caries progression in 14 volunteers [34]. An encapsulated resin-modified glass ionomer provided protection against secondary caries in 20 volunteers [41]. In the present study, CFU counts for total streptococci, mutans streptococci and lactobacilli were not significantly decreased in biofilms on the NACP nanocomposite, compared to control composite. This is expected because calcium phosphate composites are not known to have

antibacterial activity. The purpose of using calcium phosphate composite was the release of Ca and P ions to combat dental caries. However, future study is needed to investigate NACP nanocomposite containing antibacterial agents to inhibit biofilm growth and caries formation in an in situ model [48,49]. The relatively large scatter in the CFU data in Fig. 3 was likely related to the different volunteers with different biofilm compositions and dietary habits. The CFU mean values and standard deviations in the present study are similar to those reported in previous studies [39,41]. Furthermore, because fluoride is widely used throughout the populations, future study should compare the caries-inhibition efficacy of NACP nanocomposite with a fluoride-releasing restorative in an in situ investigation.

Biofilms on NACP nanocomposite restorations in situ had Ca and P ion concentrations that were significantly higher than those on the control composite. This provided a large ion reservoir in biofilms and plaques that could be released during acid attacks. Furthermore, the NACP nanocomposite was “smart” and greatly increased the ion release at a cariogenic pH 4, when these ions would be most needed to inhibit caries. Previous studies demonstrated that the released ions were able to diffuse deep into the tooth structure, and these mineral ions were transferred into the body of lesions to restore the mineral lost due to acid attacks [23]. Dental caries is a dietary carbohydrate-modified bacterial infectious disease, in which acidogenic bacteria ferment carbohydrates and produce organic acids [47,50]. Following a sucrose rinse, the plaque pH drops into the cariogenic area of 5.5 to 4, and then increases back to above 5.5 after the bacteria have completed their metabolization and the saliva has buffered the acid. Therefore, the triggered Ca and P ion release at local cariogenic pH conditions is beneficial to inhibit caries. This is manifested by the much smaller enamel lesions around the NACP nanocomposite than those around the control composite.

The present study focused on caries formation at the restoration-enamel margins, hence the mineral content was measured for the enamel region up to a distance of 250  $\mu\text{m}$  from the restoration-enamel interface. In enamel regions at four different distances of 0-50, 50-100, 100-150 and 150-200  $\mu\text{m}$  from the interface, the NACP nanocomposite imparted the same protection to enamel against mineral loss. Previous studies quantified the caries-inhibiting effect of CaP composites using remineralization, R [44]. To illustrate the calculation of R, assume that the mineral loss in the tooth structure around a CaP composite is  $!Z_{\text{CaP}}$ , and the mineral loss around a non-releasing control restoration is  $!Z_{\text{Control}}$ . Remineralization is defined as:  $R = (!Z_{\text{Control}} - !Z_{\text{CaP}}) / !Z_{\text{Control}}$  [44]. For example, if a CaP composite has no caries-inhibition capability, hence  $!Z_{\text{CaP}} = !Z_{\text{Control}}$ , then  $R = 0\%$ . On the other hand, if a CaP composite completely inhibits the caries formation, yielding  $!Z_{\text{CaP}} = 0$ , then  $R = 100\%$ . In the present study, the average  $!Z$  in the 0-250  $\mu\text{m}$  enamel region,  $!Z_{\text{NACPnanocomposite}} = 13.8 \mu\text{m}$ , and  $!Z_{\text{ControlComposite}} = 33.5 \mu\text{m}$ . This resulted in a remineralization  $R = 59\%$ . This extent of remineralization was higher than the R values of 13-38% for traditional CaP restoratives previously measured using the same quantitative microradiographic method [44]. It would be interesting to investigate if R can be further increased by incorporating antibacterial agents into the NACP nanocomposite to combine the remineralizing and antibacterial capabilities to synergistically inhibit caries in situ.

The caries-inhibition results of this study, together with the previously-reported acid neutralization and good mechanical properties [27,28], indicate that the NACP nanocomposite is promising for dental restorations to inhibit secondary caries. For example, NACP nanocomposite is promising for high-caries-risk patients, for those with dry mouth such as senior patients, and in cavities where complete removal of caries tissues is contra-indicated. There is an increasing interest in less removal of tooth structure and minimal-intervention dentistry [51], which could leave behind more carious tissues in the prepared tooth cavity. Furthermore, atraumatic restorative treatments (ART) do not remove caries completely [52]. The NACP nanocomposite could be useful to release Ca and P ions and

remineralize the remaining tooth lesions in the cavity. Many developing countries have a prevalence of dental caries. Even in the USA, people of certain ethnicity and poverty levels have a high incidence of untreated caries. NACP nanocomposite with an effective caries-inhibition efficacy could help address these problems and potentially have a vast international market. In addition, NACP nanoparticles could be incorporated into adhesives, inlay and crown cements, and orthodontic bracket cements with caries-inhibiting benefits. Further studies are needed to investigate these applications.

## 5. Conclusions

Novel NACP nanocomposite was demonstrated to be effective in inhibiting secondary caries in a human *in situ* model for the first time. The NACP nanocomposite significantly increased the Ca and P ion concentrations in the biofilms *in situ*. The release of Ca and P ions from the NACP nanocomposite was significantly increased at cariogenic low pH, when these ions were most needed to inhibit caries. Enamel sections showed typical subsurface lesions at the margins next to the control composite. However, the enamel lesions were greatly reduced around the NACP nanocomposite. In a 0-250  $\mu\text{m}$  region in enamel from the composite-enamel interface, NACP nanocomposite reduced the enamel mineral loss to nearly 1/3 of the mineral loss around the control composite. In view of recurrent caries at the tooth-restoration margins as the main factor for restoration failure, the NACP nanocomposite with an effective cariesinhibiting capability is promising for a wide range of dental restorations.

## Acknowledgments

We are grateful to Dr. Laurence C. Chow for fruitful Discussions. We thank Drs. Shozo Takagi, Gary E. Schumacker, Anthony A. Giuseppetti, Bill D. Schmuck, Clifton M. Carey, Kathleen M. Hoffman and Drago Skrtic for experimental help, and Esstech (Essington, PA) for generously donating the materials. The *in situ* experiment with volunteers was supported by the laboratory of LKAR. The materials development, specimen preparation, data measurement and analyses were supported by NIH R01DE17974 and R01DE14190 (HX) and the University of Maryland School of Dentistry seed grant (HX). MASM acknowledges a scholarship from the Coordination for Improvement of Higher Education/Fulbright Doctoral Program BEX 0523/11-9.

## References

1. Bayne SC, Thompson JY, Swift EJ, Stamatiades P, Wilkerson M. A characterization of first-generation flowable composites. *J Am Dent Assoc.* 1998; 129:567–577. [PubMed: 9601169]
2. Ruddell DE, Maloney MM, Thompson JY. Effect of novel filler particles on the mechanical and wear properties of dental composites. *Dent Mater.* 2002; 18:72–80. [PubMed: 11740967]
3. Watts DC, Marouf AS, Al-Hindi AM. Photo-polymerization shrinkage-stress kinetics in resin-composites: methods development. *Dent Mater.* 2003; 19:1–11. [PubMed: 12498890]
4. Ferracane JL. Hygroscopic and hydrolytic effects in dental polymer networks. *Dent Mater.* 2006; 22:211–222. [PubMed: 16087225]
5. Krämer N, García-Godoy F, Reinelt C, Frankenberger R. Clinical performance of posterior compomer restorations over 4 years. *Am J Dent.* 2006; 19:61–66. [PubMed: 16555660]
6. Samuel SP, Li S, Mukherjee I, Guo Y, Patel AC, Baran GR, Wei Y. Mechanical properties of experimental dental composites containing a combination of mesoporous and nonporous spherical silica as fillers. *Dent Mater.* 2009; 25:296–301. [PubMed: 18804855]
7. Carvalho RM, Manso AP, Geraldini S, Tay FR, Pashley DH. Durability of bonds and clinical success of adhesive restorations. *Dent Mater.* 2012; 28:72–86. [PubMed: 22192252]
8. Xu X, Ling L, Wang R, Burgess JO. Formation and characterization of a novel fluoride-releasing dental composite. *Dent Mater.* 2006; 22:1014–1023. [PubMed: 16378636]
9. Drummond JL. Degradation, fatigue, and failure of resin dental composite materials. *J Dent Res.* 2008; 87:710–719. [PubMed: 18650540]



10. Spencer P, Ye Q, Park JG, Topp EM, Misra A, Marangos O, Wang Y, Bohaty BS, Singh V, Sene F, Eslick J, Camarda K, Katz JL. Adhesive/dentin interface: The weak link in the composite restoration. *Annals of Biomed Eng.* 2010; 38:1989–2003.
11. Wan Q, Sheffield J, McCool J, Baran GR. Light-curable dental composites designed with colloidal crystal reinforcement. *Dent Mater.* 2008; 24:1694–1701. [PubMed: 18499245]
12. Watts DC, Issa M, Ibrahim A, Wakiaga J, Al-Samadani K, Al-Azraqi M, et al. Edge strength of resin-composite margins. *Dent Mater.* 2008; 24:129–133. [PubMed: 17580089]
13. Imazato S. Bioactive restorative materials with antibacterial effects: new dimension of innovation in restorative dentistry. *Dent Mater J.* 2009; 28:11–19. [PubMed: 19280964]
14. Walter R, Swift EJ Jr, Ritter AV, Bartholomew WW, Gibson CG. Dentin bonding of an etch-and-rinse adhesive using self- and light-cured composites. *Am J Dent.* 2009; 22:215–218. [PubMed: 19824557]
15. Guo G, Fan Y, Zhang JF, Hagan JL, Xu X. Novel dental composites reinforced with zirconia–silica ceramic nanofibers. *Dent Mater.* 2012; 28:360–368. [PubMed: 22153326]
16. Sakaguchi RL. Review of the current status and challenges for dental posterior restorative composites: clinical, chemistry, and physical behavior considerations. *Dent Mater.* 2005; 21:3–6. [PubMed: 15680996]
17. Ferracane JL. Resin composite - State of the art. *Dent Mater.* 2011; 27:29–38. [PubMed: 21093034]
18. Demarco FF, Correa MB, Cenci MS, Moraes RR, Opdam NJM. Longevity of posterior composite restorations: Not only a matter of materials. *Dent Mater.* 2012:87–101. [PubMed: 22192253]
19. Mjör IA, Moorhead JE, Dahl JE. Reasons for replacement of restorations in permanent teeth in general dental practice. *International Dent J.* 2000; 50:361–366.
20. Frost PM. An audit on the placement and replacement of restorations in a general dental practice. *Prim Dent Care.* 2002; 9:31–36. [PubMed: 11901789]
21. Jokstad A, Bayne S, Blunck U, Tyas M, Wilson N. Quality of dental restorations. FDI Commision Projects 2-95. *International Dent J.* 2001; 51:117–158.
22. Dickens SH, Flaim GM, Takagi S. Mechanical properties and biochemical activity of remineralizing resin-based Ca-PO<sub>4</sub> cements. *Dent Mater.* 2003; 19:558–566. [PubMed: 12837405]
23. Langhorst SE, O'Donnell JNR, Skrtic D. In vitro remineralization of enamel by polymeric amorphous calcium phosphate composite: Quantitative microradiographic study. *Dent Mater.* 2009; 25:884–891. [PubMed: 19215975]
24. Brown ML, Davisb HB, Tufekci E, Crowe JJ, Covell DA, Mitchell JC. Ion release from a novel orthodontic resin bonding agent for the reduction and/or prevention of white spot lesions - An in vitro study. *Angle Orthod.* 2011; 81:1014–1020. [PubMed: 22007662]
25. Qi YP, Li N, Niu LN, Primus CM, Ling JQ, Pashley DH, Tay FR. Remineralization of artificial dentinal caries lesions by biomimetically modified mineral trioxide aggregate. *Acta Biomater.* 2012; 8:836–842. [PubMed: 22085925]
26. LeGeros, RZ. Calcium phosphates in oral biology and medicine. Myers, HM., editor. Vol. Chapters 3-4. Basel, Switzerland: S. Karger; 1991.
27. Xu HHK, Moreau JL, Sun L, Chow LC. Nanocomposite containing amorphous calcium phosphate nanoparticles for caries inhibition. *Dent Mater.* 2011; 27:762–769. [PubMed: 21514655]
28. Moreau JL, Sun L, Chow LC, Xu HHK. Mechanical and acid neutralizing properties and inhibition of bacterial growth of amorphous calcium phosphate dental nanocomposite. *J Biomed Mater Res.* 2011; 98B:80–88.
29. Xu HHK, Sun L, Weir MD, Antonucci J, Takagi S, Chow LC. Nano DCPA-whisker composites with high strength and Ca-PO<sub>4</sub> release. *J Dent Res.* 2006; 85:722–27. [PubMed: 16861289]
30. Sun L, Chow LC. Preparation and properties of nano-sized calcium fluoride for dental applications. *Dent Mater.* 2008; 24:111–116. [PubMed: 17481724]
31. Xu HHK, Weir MD, Sun L. Dental nanocomposites with Ca-PO<sub>4</sub> release: Effects of reinforcement, dicalcium phosphate particle size and silanization. *Dent Mater.* 2007; 23:1482–1491. [PubMed: 17339048]

32. Skrtic D, Antonucci JM, Eanes ED. Improved properties of amorphous calcium phosphate fillers in remineralizing resin composites. *Dent Mater.* 1996; 12:295–301. [PubMed: 9170997]
33. Tenuta LMA, Del Bel Cury AA, Bortolin MC, Vogel GL, Cury JA. Ca, Pi, and F in the fluid of biofilm formed under sucrose. *J Dent Res.* 2006; 85:834–838. [PubMed: 16931867]
34. Cenci MS, Tenuta LMA, Pereira-Cenci T, Del Bel Cury AA, ten Cate JM, Cury JA. Effect of microleakage and fluoride on enamel-dentine demineralization around restorations. *Caries Res.* 2008; 42:369–379. [PubMed: 18753749]
35. Paradella TC, Koga-Ito CY, Jorge AOC. Ability of different restorative materials to prevent in situ secondary caries: analysis by polarized light-microscopy and energy dispersive X-ray. *Eur J Oral Sci.* 2008; 116:375–380. [PubMed: 18705806]
36. Lima JP, Sampaio de Melo MA, Borges FM, Teixeira AH, Steiner-Oliveira C, Nobre Dos Santos M, Rodrigues LK, Zanin IC. Evaluation of the antimicrobial effect of photodynamic antimicrobial therapy in an in situ model of dentine caries. *Eur J Oral Sci.* 2009; 117:568–574. [PubMed: 19758254]
37. Deng DM, ten Cate JM. Caries-preventive agents induce remineralization of dentin in a biofilm model. *Caries Res.* 2005; 39:216–223. [PubMed: 15914984]
38. Hara AT, Turssi CP, Ando M, González-Cabezas C, Zero DT, Rodrigues AL Jr, Serra MC, Cury JA. Influence of fluoride-releasing restorative material on root dentine secondary caries in situ. *Caries Res.* 2006; 40:435–9. [PubMed: 16946613]
39. Aires CP, Del Bel Cury AA, Tenuta LMA, Klein MI, Koo H, Duarte S, Cury JA. Effect of starch and sucrose on dental biofilm formation and on root dentine demineralization. *Caries Res.* 2008; 42:380–386. [PubMed: 18781066]
40. Cenci MS, Pereira-Cenci T, Cury JA, ten Cate JM. Relationship between gap size and dentine secondary caries formation assessed in a microcosm biofilm model. *Caries Res.* 2009; 43:97–102. [PubMed: 19321986]
41. Sousa RP, Zanin IC, Lima JP, Vasconcelos SM, Melo MA, Beltrão HC, Rodrigues LK. In situ effects of restorative materials on dental biofilm and enamel demineralisation. *J Dent.* 2009; 37:44–51. [PubMed: 19026481]
42. Cury JA, do Amaral RC, Tenuta LMA, Del Bel Cury AA, Tabchoury CPM. Low fluoride toothpaste and deciduous enamel demineralization under biofilm accumulation and sucrose exposure. *Eur J Oral Sci.* 2010; 118:370–375. [PubMed: 20662910]
43. Schmuck BD, Carey CM. Improved contact x-ray microradiographic method to measure mineral density of hard dental tissues. *J Res Natl Inst Stand Technol.* 2010; 115:75–83. [PubMed: 21546983]
44. Dickens SH, Flaim GM. Effect of a bonding agent on in vitro biochemical activities of remineralizing resin-based calcium phosphate cements. *Dent Mater.* 2008; 24:1273–1280. [PubMed: 18359510]
45. Cheng L, Weir MD, Xu HHK, Kraigsley AM, Lin NJ, Lin-Gibson S, Zhou X. Antibacterial and physical properties of calcium-phosphate and calcium-fluoride nanocomposites with chlorhexidine. *Dent Mater.* 2012; 28:573–583. [PubMed: 22317794]
46. Xu HHK, Weir MD, Sun L, Moreau JL, Takagi S, Chow LC, Antonucci JM. Strong nanocomposites with Ca, PO<sub>4</sub> and F release for caries inhibition. *J Dent Res.* 2010; 89:19–28. [PubMed: 19948941]
47. ten Cate JM. Biofilms, a new approach to the microbiology of dental plaque. *Odontology.* 2006; 94:1–9. [PubMed: 16998612]
48. Imazato S. Review: Antibacterial properties of resin composites and dentin bonding systems. *Dent Mater.* 2003; 19:449–457. [PubMed: 12837391]
49. Xie D, Weng Y, Guo X, Zhao J, Gregory RL, Zheng C. Preparation and evaluation of a novel glass-ionomer cement with antibacterial functions. *Dent Mater.* 2011; 27:487–496. [PubMed: 21388668]
50. Featherstone JDB. The continuum of dental caries - Evidence for a dynamic disease process. *J Dent Res.* 2004; 83:C39–C42. [PubMed: 15286120]
51. Tyas MJ, Anusavice KJ, Frencken JE, Mount GJ. Minimal intervention dentistry - a review FDI commission project 1-97. *International Dent J.* 2000; 50:1–12.

52. Frencken JE, van't Hof MA, van Amerongen WE, Holmgren CJ. Effectiveness of single-surface ART restorations in the permanent dentition: a meta-analysis. *J Dent Res.* 2004; 83:120–123. [PubMed: 14742648]
53. Chow LC, Takagi S, Shih S. Effect of a two-solution fluoride mouthrinse on remineralization of enamel lesions in vitro. *J Dent Res.* 1992; 71:443–447. [PubMed: 1315346]

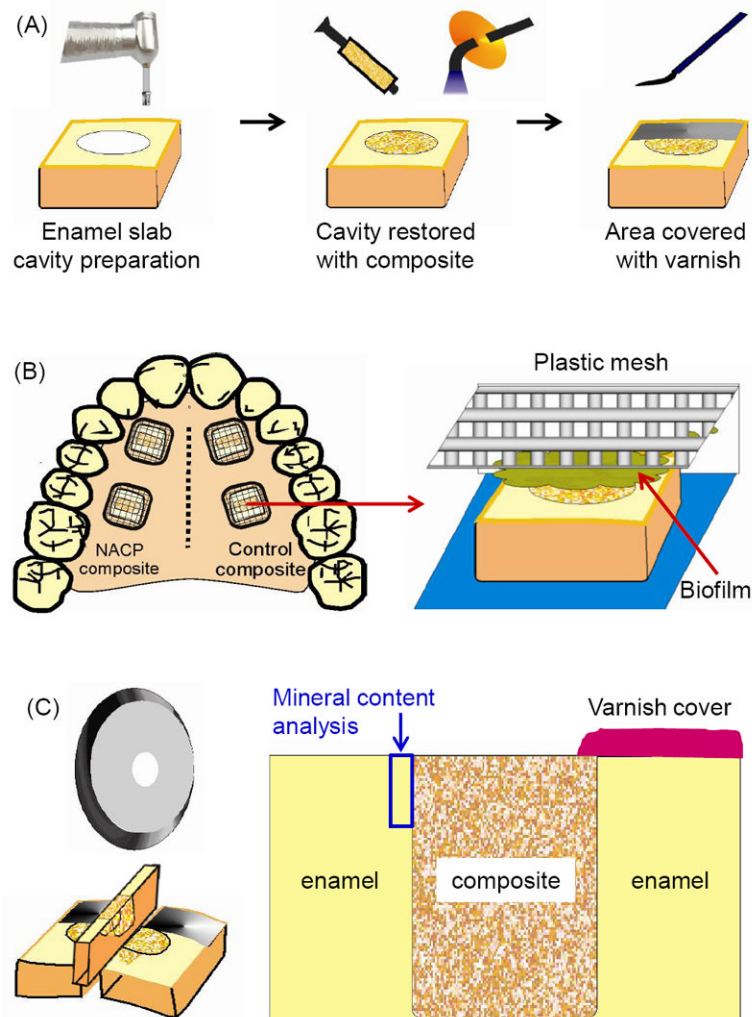


**Figure [1].**

Schematic of in situ experiment. (A) One hundred bovine enamel slabs of 5×5×2 mm were obtained. A cavity of 2 mm in diameter and 1.5 mm in depth was prepared and subsequently restored with the test composite. Varnish was applied on one side. (B) 25 volunteers wore palatal devices each containing four slabs: two filled with NACP nanocomposite on one side, and two filled with control composite on the other side. A plastic mesh with 1 mm space protected the biofilm. (C) Enamel slabs were cut to obtain sections of 110-130 μm thickness. Contact microradiographs were obtained to measure the enamel mineral content at the margins.

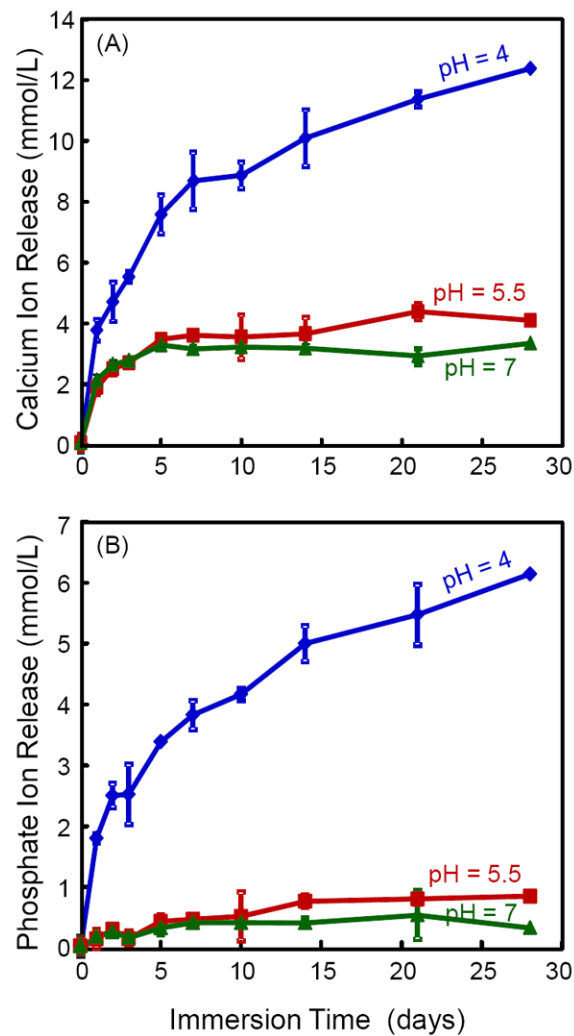


**Figure [2].**

Calcium and phosphate ion releases from NACP nanocomposite immersed in solutions of pH 4, pH 5.5, and pH 7 (mean  $\pm$  sd; n = 5). Ion releases at pH 4 were higher than those at pH 5.5 and 7 ( $p < 0.05$ ). The NACP nanocomposite was “smart” and greatly increased the ion release at cariogenic pH 4, when these ions were most needed to inhibit caries.



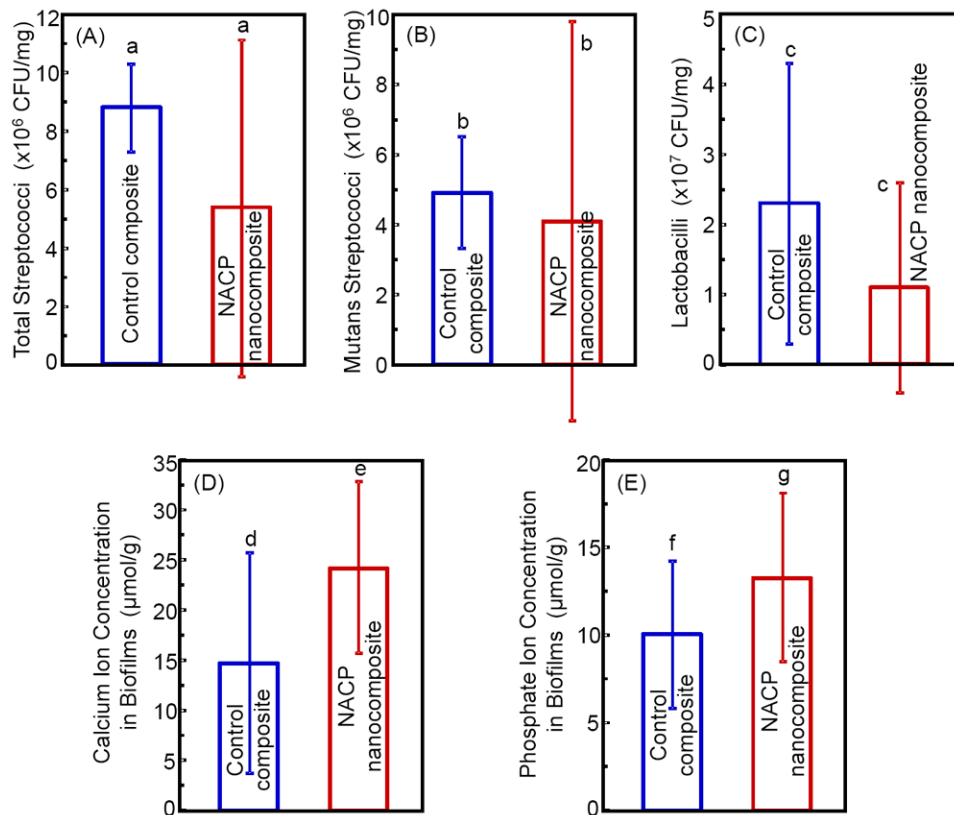


**Figure [3].**

Analyses of oral biofilms harvested from the volunteers: (A) Total streptococci, (B) mutans streptococci, (C) lactobacilli, (D) Ca and (E) P ion concentrations (mean  $\pm$  sd; n = 25). In each plot, dissimilar letters indicate values significantly different from each other (p < 0.05). Biofilm CFU counts were not significantly different on the two composites (p > 0.1). The biofilms on NACP nanocomposite contained significantly more Ca and P ions than those on control composite (p < 0.05).

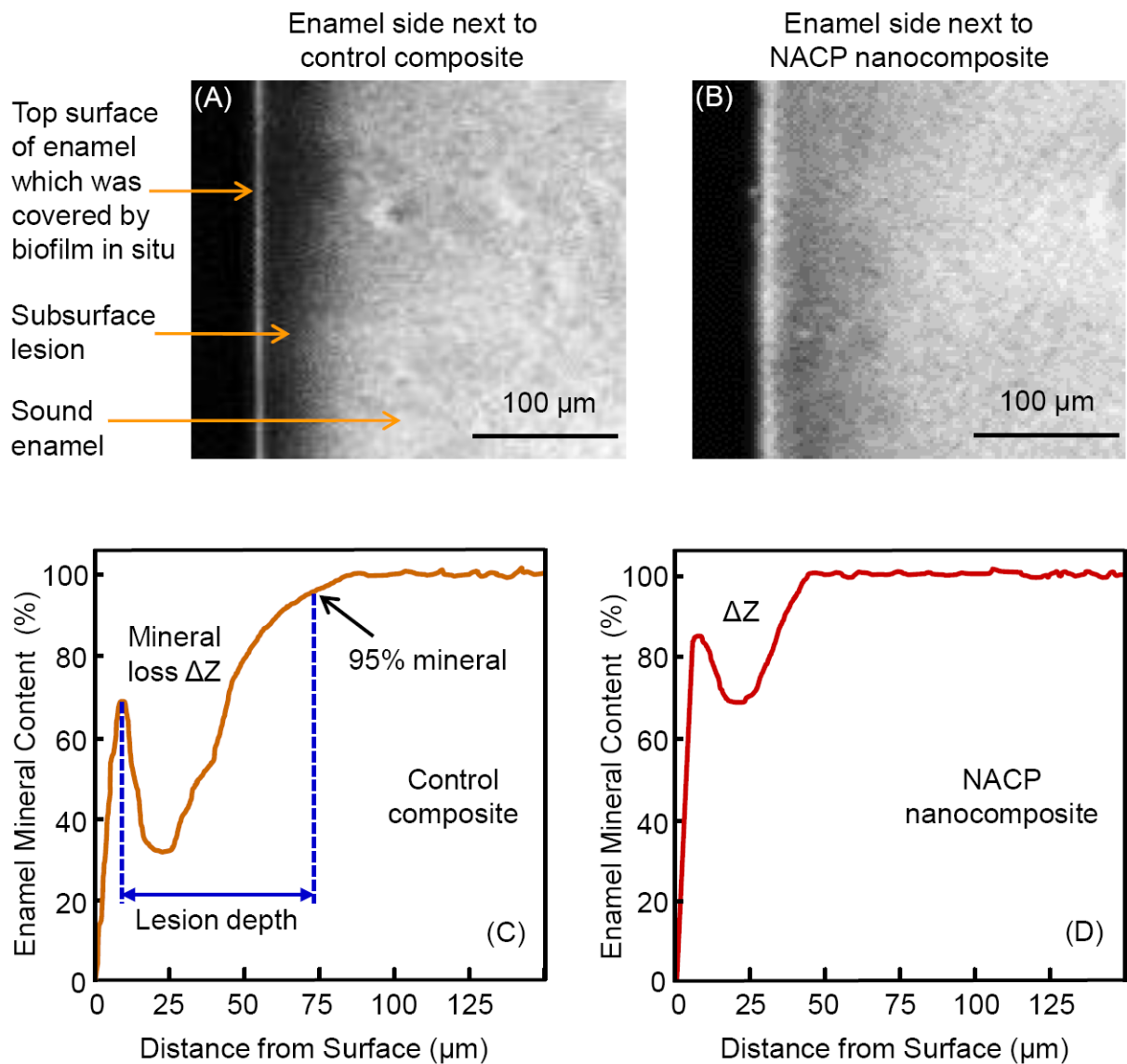


**Figure [4].**

Transverse microradiography analysis. Representative images showed subsurface enamel lesions around (A) control composite, and (B) NACP nanocomposite. (C) The lesion depth was defined as the distance from the first bump on the mineral profile to the location which reached a mineral content of 95% of sound enamel, following a previous study [22,23,53]. (D) Exposed enamel (no varnish cover) under biofilms in situ had much less lesion around NACP nanocomposite than that around control composite in (C).

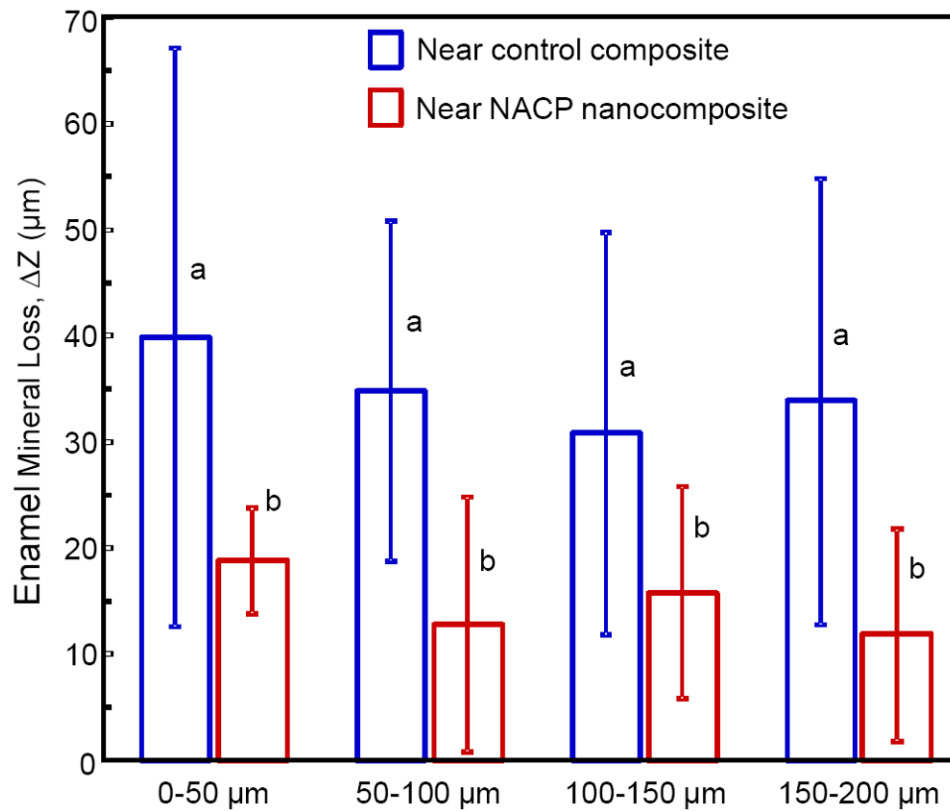


**Figure [5].** Enamel mineral loss around NACP nanocomposite and control composite versus the distance from the enamel-composite interface. The numbers at the x-axis refer to the location in enamel from the interface at four different distances. For each composite, the distance did not significantly change ! Z ( $p > 0.1$ ). At each distance, enamel mineral loss was much less around NACP nanocomposite than control composite (mean  $\pm$  sd;  $n = 25$ ). Values with dissimilar letters are significantly different from each other ( $p < 0.05$ ).

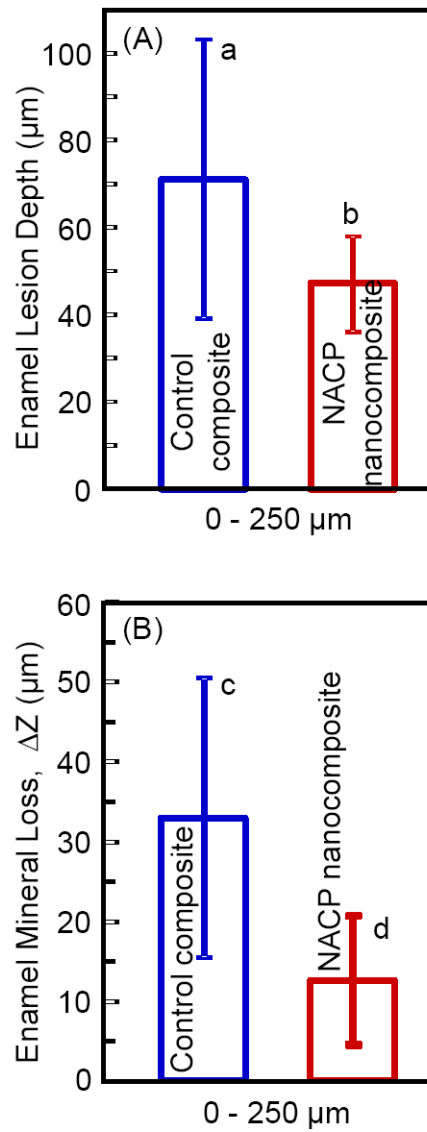


**Figure [6].**

The enamel region of 0-250 μm from the enamel-composite interface was analyzed to obtain the average lesion depth and mineral loss in this region. (A) Enamel lesion depth, and (B) mineral loss (mean ± sd; n = 25). Enamel mineral loss around the NACP nanocomposite was reduced to nearly 1/3 of the mineral loss around the control composite ( $p < 0.05$ ).